To cite this article: GUO S Z, MA J, LI Z Y, et al. Design and swimming test of myliobatid-inspired robot[J/OL]. Chinese Journal of Ship Research, 2022, 17(4). http://www. ship-research. com/en/article/doi/10.19693/j. issn. 1673-3185.02497.

DOI: 10.19693/j.issn.1673-3185. 02497

Design and swimming test of myliobatid-inspired robot

GUO Songzi[*1], *MA Jun*[2], *LI Zhiyin*[1], *ZHANG Jinhua*[3]

1 China Ship Development and Design Center, Wuhan 430064, Hubei, China

2 Project Management Center, Naval Armament Department of PLAN, Beijing 100071, China

3 School of Mechanical Engineering, Xi'an Jiaotong University, Xi'an 710049, Shaanxi, China

Abstract: [**Objectives**] Over millions of years of natural selection, fish have evolved various types of swimming modes with various advantages in efficiency, motility, and tranquility, which makes them become ideal biological objects on which autonomous underwater vehicles (AUVs) can be modeled. In order to develop a brand-new AUV with lower noise and higher mobility, this paper puts forward a design for a myliobatid-inspired robot actuated by flexible pectoral fins. [**Methods**] The manufacturing process and actuating method of the prototype are illustrated in detail. In order to test the maximum speed and mobility of the prototype, a series of swimming tests are carried out. [**Results**] The experimental results show that the prototype can complete a variety of maneuvers in water, including rolling, small radius steering, and hovering, and its maximum swimming speed can reach 1.9 times the body length per second (about 0.73 m/s). [**Conclusions**] This paper outlines the preliminary design and swimming tests of a myliobatid-inspired robot and provides a reference for the design of the next generation of AUVs.

Key words: autonomous underwater vehicle (AUV); bio-inspired robot; swimming test

CLC number: U662.2

0 Introduction

With the ongoing growth of the industrial economy, various land resources such as oil, natural gas, and rare metals become increasingly scarce. As land resources gradually deplete, the exploitation and utilization of marine resources become one of the imperatives for human beings. In order to serve the needs of ocean exploration and resource exploitation, countries have been intensifying their research on autonomous underwater vehicles (AUVs) in recent decades, which thus leads to the exponential growth of AUVs. Adopting the conventional propulsion system composed of propellers mostly, traditional AUVs feature a compact and simple structure, high reliability, and excellent tightness. However, due to massive cavitation and vortices generated by propellers in operation, traditional AUVs produce too much noise that brings significant disturbances to the environment during work, which is harmful to their operation in environments with a high demand for tranquility [1]. In addition, the propeller-based driver cannot generate vector propulsive force, which results in poor maneuverability of the body during its underwater movement. As a result, it is difficult to be applied to conduct the increasingly complex underwater exploration.

In order to explore other efficient and flexible underwater propulsion modes different from propeller propulsion, engineers both in China and abroad focused on various fishes in the ocean to get inspiration from their swimming modes and expected to shed light on the development of new high-performance AUVs by imitating the morphological characteristics and swimming mechanism of marine organisms in the nature [2]. As a typical fish that uses central fins to move ahead, myliobatidae fishes have excellent hydrodynamic shapes. Generating

Received: 2021 – 08 – 20 **Accepted**: 2022 – 01 – 11

Authors: GUO Songzi , male, born in 1995, master degree, engineer.

MA Jun, male, born in 1979, master degree, engineer

LI Zhiyin,male, born in 1980 , master degree, senior engineer

ZHANG Jinhua, male, born in 1972, PhD., professor. Research interest: soft robot. E-mail: jjshua@mail.xjtu.edu.cn

***Corresponding author**: GUO Songzi

propulsive force and additional control torque by flapping their central fins, myliobatidae fishes display strong flexibility and stability in underwater movement, which makes them adapt to long-distance migration in the ocean and capable of low-speed flexible maneuvers. Accordingly, myliobatidae fishes that move ahead by flapping their central fins have become the model constantly imitated and studied by engineers in designing a new generation of underwater propellers.

Early flap-driven bionic robot fishes mostly feature rigid designs and show high structural reliability and large propulsive force. But they also have many shortcomings, such as bulky support skeletons, low swimming efficiency, and poor environmental adaptability, which make them almost incompetent for the increasingly complex ocean exploration. Early in 2004, Japanese scholars developed the prototype of a bionic fish driven by flapping pectoral fins. The fish was supported by a rigid skeleton with its fin surfaces made of flexible silica gel plates. With a length of about 650 mm, a wingspan of 500 mm, and a weight of 640 g, the prototype, driven by a servo motor, could reach a maximum swimming speed of one time the body length per second. Afterward, Chinese scholars Xu et al. [3] and Gao et al. [4] adopted a similar pectoral fin structure, designed the manta ray-inspired robot fish BH-RAY3 driven by flapping the rigid pectoral fins on both sides, and studied its basic propulsion mechanism through hydrodynamic tests. With the manta ray as a bionic object, Festo company (Germany) also designed the manta-inspired robot fish AquaRay driven by a rigid support motor, and the fish could glide in the water due to the exquisite structural design and control method, which greatly improved the swimming efficiency of the robot fish. EvoLogics developed a manta-inspired robot fish with an artificial jet propeller as the driver. The MantaBot prototype jointly developed by the University of Virginia and the US Naval Research Laboratory followed the idea of rigid-flexible coupling and controlled the swing of the pectoral fins through the expansion and contraction of a rigid tension mechanism built in the flexible pectoral fins, which better simulated the motion state of a real manta ray [5].

As relevant research deepens, bionic fish robots adopting a fully flexible design have gained wide attention from scholars because of their light structures, strong environmental adaptability, and high swimming efficiency. Chew et al. [6] found through hydrodynamic tests that the passive large deformation of the outer side of the bionic pectoral fins contributed to higher propulsion efficiency, and they produced fully flexible bionic pectoral fins with fin rays and fin surfaces made of flexible materials [7]. According to the test results, the prototype MantaDroid driven by the flexible pectoral fins reached a relatively high underwater swimming speed of up to 1.7 times the body length per second.

By summarizing the status quo of the research on flap-driven bionic fishes both in China and abroad in recent years, it is found that the research focus has changed from rigid fin drive to flexible fin drive, and active deformation control of multiple degrees of freedom has changed to passive deformation design conforming to the surrounding water environment. In addition, the robot fish bodies have evolved from the similarity of body shape to that of motion deformation and generally achieved the imitation of the shape and attitude of the bionic objects. The existing prototypes of flap-driven robot fishes can perform simple motion functions including linear swimming and fixed-depth cruising, but their underwater maneuverability remains far from that of real fishes, which greatly limits their application in engineering [8].

In view of these shortcomings, this paper takes the development of a flap-driven bionic fish with a fast swimming speed and high maneuverability as a research objective and puts forward a design scheme for a bionic robot (hereinafter referred to as robot fish) that is driven by flapping the flexible pectoral fins. Furthermore, the paper completes the production and swimming test of relevant prototypes. The completed robot fish prototype (XJRoman) has a total length of 385 mm, a wingspan of 550 mm, and a total mass of about 720 g. It takes full advantage of the streamlined shape of a real eagle ray to reduce the resistance from the water flow during swimming. Through synchronous or asynchronous flaps of the flexible bionic pectoral fins on both sides, the robot fish can achieve flexible movement with multiple degrees of freedom and thus exhibit excellent underwater maneuverability.

1 Design and production of the flap-driven myliobatid-inspired robot fish

1.1 Overall design of the robot fish

After the real size and morphological characteris-

tics of a juvenile eagle ray are fully analyzed, the prototype of a myliobatid-inspired robot fish is designed and presented in Fig. 1. With a streamlined contour, the prototype has a total length of 385 mm and a wingspan of 550 mm. Driven by a pair of central flexible bionic pectoral fins, it controls the pitch swimming attitude through the horizontal stern rudder at the rear end. The middle cabin of the robot fish is placed with a variety of electronic devices, including a motion control panel, an inertial measurement unit (IMU), and a water pressure sensor, so as to provide control of and real-time data feedback on the attitude and depth information of the prototype during its swimming.

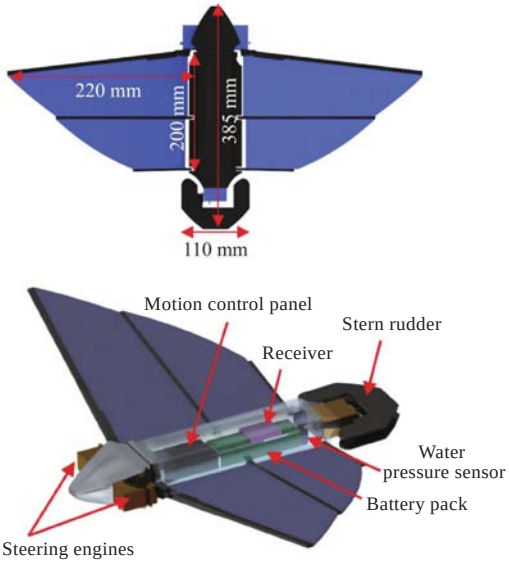

Fig. 1 Design scheme of the prototype of the myliobatid-inspired robot fish

1.2 Structural design and production of flap-driven bionic pectoral fins

As bionic pectoral fins serve as the flapping propulsion device of the prototype of the myliobatid-inspired robot fish, the rationality of their structural design greatly affects the overall motion performance of the robot fish. The design of the bionic pectoral fins should not only take into account the anatomical structure characteristics of the flexible pectoral fins but also be smoothly realized and controlled [9]. To guide the structural design of the flexible pectoral fins of the myliobatid-inspired robot fish, we carry out an anatomical experiment on the pectoral fins of an eagle ray. In the shape of a pennant, the pectoral fin sample has an aspect ratio of about 2. After removing the muscle tissue structure on the surface of the pectoral fins with a surgical knife, we obtain the bone structure inside the fins, as shown in Fig. 2 (a). The structure is composed of multiple radially-arranged calcified spokes (fin rays) and soft tissues between the spokes. Specifically, each spoke is connected by multiple segments of radii through flexible joints and can rotate slightly around the flexible cartilaginous joints, which thus shows positive biological flexibility. Besides, two adjacent spokes of the pectoral fins are connected by fine and small cartilaginous joints, which strengthens the rigidity along the chord length to some extent and ensures the control of the pectoral fins over the chordwise waveform. The overall thickness of the pectoral fin sample tapers off from the root to the end, and thus its stiffness gets smaller from the inside to the outside, as shown in Fig. 2 (b).

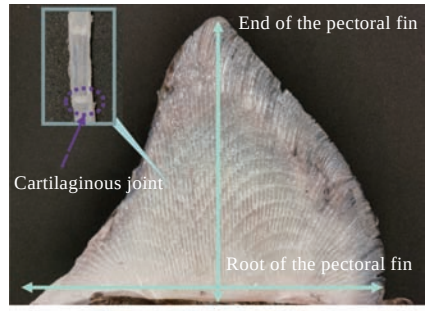

(a) Internal skeletal structure of the pectoral fin of the eagle ray

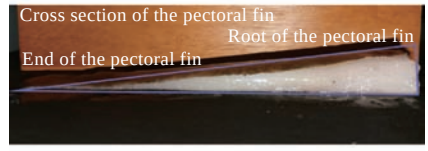

(b) Distribution of muscle tissues in the pectoral fin of the eagle ray

Fig. 2 Pectoral fin specimens of a dissected eagle ray

The above anatomical study of the pectoral fins of the eagle ray can lead to the following conclusions:

First, the pectoral fin of the eagle ray is in the shape of a pennant, with an aspect ratio of about 2. The layout of the multiple spokes inside the pectoral fins and the flexible cartilage on the spokes can ensure the biological flexibility of the pectoral fins during movement so that the eagle ray can perform complex flap-driven movements, which contributes a lot to the flexibility and stability of its movement.

Second, the non-uniform stiffness distribution of the pectoral fins along the wingspan is of great significance to their spanwise deformation when the eagle ray moves.

Therefore, in the follow-up design of the flexible pectoral fins of the myliobatid-inspired robot fish, it is necessary to fully learn from the characteristics in terms of the pennant shape of the pectoral fins, the multi-spoke layout, and the non-uniform stiffness distribution along the wingspan of the eagle ray, so

as to realize a morphological bionic design. In this way, the pectoral fins can flap back and forth periodically through a similar spoke-driven structure.

Based on the above morphological and anatomical characteristics of the pectoral fins of an eagle ray, this paper adopts the flexible bionic pectoral fins and applied them to the test prototype (XJRoman) shown in Fig. 3. The flexible bionic pectoral fin is generally composed of flexible fin surfaces and flexible fin rays. Specifically, three fin rays are arranged transversely along the body length with a spacing of 100 mm. With an included angle of 80° between the drive fin ray at the leading edge and the body length, the pectoral fin has a length of 220 mm and a width of 6 mm along the wingspan, with the thickness tapering off from 6 mm at the root to 1 mm at the end. The non-uniform stiffness distribution design of the drive fin ray can ensure the substantial deformation of the outer part of the bionic pectoral fin during the flap. Furthermore, along the wingspan, the length of the passive fin rays in the middle and the tail is 180 and 100 mm, respectively, and the width is 4 mm. In view of the demand of the bionic pectoral fin for overall flexible deformation, all three fin rays are made of high-toughness nylon (PA12) material with excellent flexibility through laser sintering, with a tensile modulus of about 1 700 MPa. The density of PA12 material is close to that of water and is about 1.13 g/cm^3, and its fracture resistance elongation can reach up to 20% along the *XY* direction. Therefore, it can meet the requirements of the flexible bionic pectoral fin for the mechanical performance of the material. The flexible fin surfaces of the bionic pectoral fin are cast with silica gel with a hardness of 30 A. Specifically, the upper fin surface has a chordwise height of 100 mm, a spanwise width of 220 mm, and a thickness of 2 mm, while the lower fin surface has a chordwise height of 100 mm, an upper-end width of 180 mm, a bottom width of 100 mm, and a thickness of 2 mm.

The whole flexible bionic pectoral fin swings back and forth through the drive fin rays at the leading edge, and the whole pectoral fin is passively driven and flaps. Besides, the bionic pectoral fin can take full advantage of the characteristics of its structural stiffness distribution when flapping and generate forward propulsive force through the terminal angle of striking formed by passive deformation. Both the fin surfaces and fin rays are made of flexible materials, and they are directly connected. Except for the driving device, the flexible bionic pectoral fin is made of zero-buoyancy flexible materials with a density close to that of water. The unilateral pectoral fin is driven by a high-performance waterproof steering engine connected to the drive fin ray, which minimizes the mechanical energy loss incurred by the driver and improves the overall working efficiency of the robot fish while reducing its overall mass.

1.3 Prototype of the robot fish

The fabricated prototype of the myliobatid-inspired robot fish (XJRoman) is shown in Fig. 4. The whole system is mainly composed of cabin parts, bionic flexible pectoral fins, drive steering engines, and internal electronic devices. Specifically, the cabin parts of the robot fish are streamlined and consist of the head cabin, middle cabin, and stern rudder. All these parts are made of PA12 material and processed by 3D printing, and they have light weight and high strength. The detachable plug-in design is adopted for the head cabin and the middle cabin. When the head cabin is buckled with the middle cabin, they become waterproof through the O-shaped seal ring. The bionic flexible pectoral fins

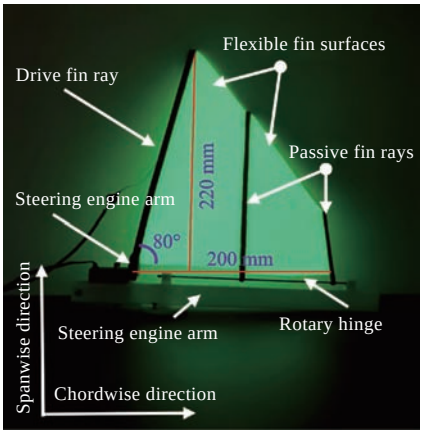

Fig. 3 A bionic pectoral fin adopted by the test prototype

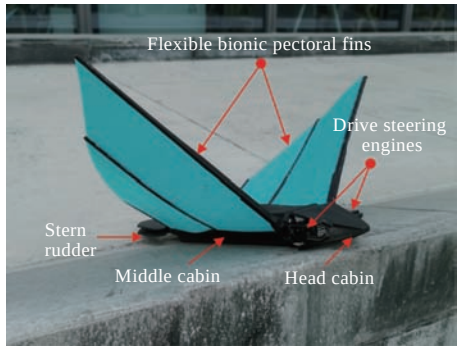

Fig. 4 Isometric view of the fabricated prototype of XJRoman

are connected with the cabin parts through a flexible rotary hinge and driven by waterproof steering engines at the head to generate propulsive force and additional control torque. The stern rudder structure of the robot fish is mainly dedicated to generating the pitch moment to adjust the pitch attitude angle. As the prototype has an overall mass of 720 g which is equivalent to its displacement, it can just stay in the water with zero buoyancy.

The electronic devices carried by the robot fish are presented in Fig. 5, and they mainly include data communication module, attitude sensing module, depth position sensing module, power supply module, and motion control panel. Composed of a STM32F407IG single-chip computer and a power management chip, the motion control panel can provide abundant interfaces for peripheral devices. It mainly serves to receive the data transmitted from various sensors, generate corresponding pulse width modulation (PWM) control signals through the timer, and adjust the swing angle and speed of the steering engines. The wireless communication module is connected to the motion control panel through the USART serial port, and it transmits the desired motion commands to the robot fish. The attitude sensing module and the depth position sensing module are connected to the motion control panel through the I^2C serial communication bus, and they control the sampling period of the data via the timer in the motion control panel.

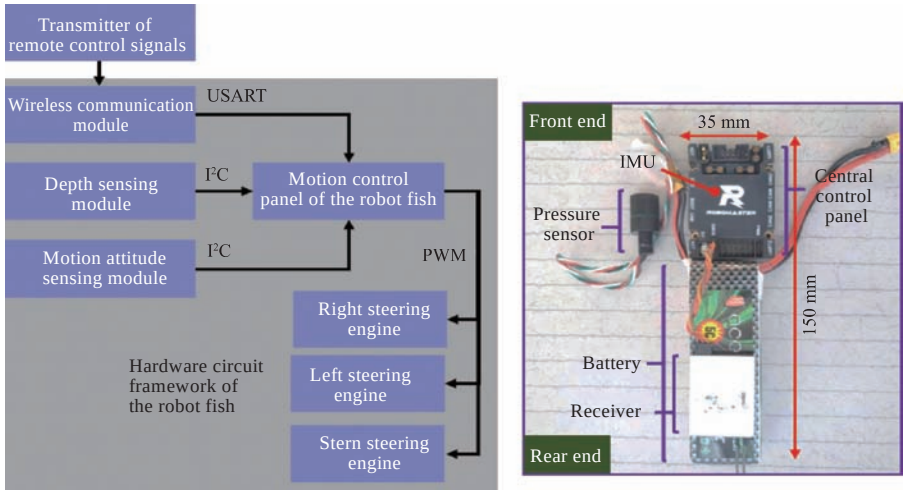

Fig. 5 Diagram of the electronic devices and connection mode of the prototype

In the nature, myliobatidae fishes switch different motion attitudes by coordinating the swinging frequency of the pectoral fins on both sides, so as to achieve flexible and stable underwater movement. For the flap-driven robot fish, the design of its control system needs not only to control the current output state of the control value of each driver but also to take into account the influence of the relationship between each output control value on the overall motion attitude of the prototype. Therefore, based on the concept of biological hierarchical control, this paper adopts the underlying drive of a central pattern generator (CPG) to control the output angle and coupling relationship of the driver corresponding to the pectoral and tail fins on both sides. The schematic diagram of the CPG underlying drive control method of the test prototype is presented in Fig. 6, and the mathematical expression describing the dynamic characteristics of CPG is as follows:

$$\begin{cases} \dot{a}_i = \gamma_i(A_i - a_i) \\ \dot{b}_i = \eta_i(B_i - b_i) \\ \dot{x}_i = 2\pi f_i + \sum_{j \in T_i} \mu_{ij}(x_j - x_i - \varphi_{ij}) \\ \theta_i = b_i + a_i \cos(x_i) \end{cases} \tag{1}$$

where a_i, b_i, and x_i are the state variables, and they represent the current amplitude, offset, and phase of the i-th oscillator, respectively; i =1, 2, and 3 represent the phase oscillators corresponding to the left steering engine, right steering engine, and stern steering engine of the myliobatid-inspired robot fish, respectively; A_i and B_i represent the expected amplitude and the expected offset of the i-th oscillator, respectively; γ_i and η_i represent the convergence coefficient of amplitude and offset, respectively, and they determine the speed at which the state variables a_i and b_i converge to the expected value; f_i represents the frequency at which the oscillator generates rhythm signals; μ_{ij} represents the coupling coefficient between the i-th and the j-th oscillators, and

it determines the coupling strength between the corresponding oscillators; φ_{ij} represents the latching phase difference between the i-th and the j-th oscillators; θ_{ij} represents the angle of the steering engine finally output by the i-th phase oscillator. In addition, by controlling the CPG network entry, the upper proportion-integration-differentiation (PID) controller can realize coordinated control among all drivers.

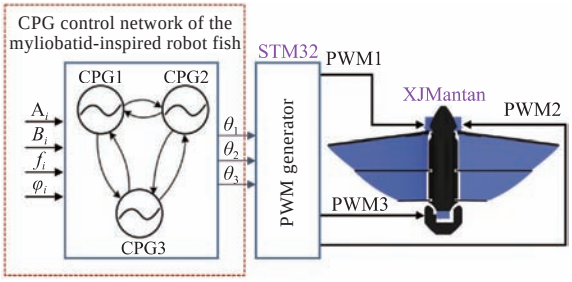

Fig. 6 Schematic diagram of the CPG underlying drive control method of the prototype

The PID1 controller takes the yaw angle collected by IMU integrated in the central control panel as the feedback signal and controls the swimming direction by controlling the difference between the flapping frequency of the left and right pectoral fins, namely, f_1 and f_2. PID2 controller takes the angle of pitch collected by the IMU as the feedback signal and controls the swimming depth of the robot fish by adjusting φ_3.

2 Swimming performance test of the prototype

2.1 Test environment and data processing

The prototype of the myliobatid-inspired robot fish (XJRoman) is tested in terms of its swimming performance in a water area with a size of 50 m × 21 m × 2 m (Fig. 7). In the test, we use a GoPro-Hero8 waterproof camera with a resolution of 4K to capture the motion of the prototype at 60 frames per second and then work out the average swimming speed of the robot fish via the Adobe Premiere frame processing software.

Fig. 7 Test environment for the swimming performance test on the prototype

2.2 Swimming speed test

By observing the swimming attitude of the eagle ray, it is found that the eagle ray mainly adjusts its swimming attitude and speed by changing the flapping frequency of the pectoral fins. In addition, it is found through the hydrodynamic test on the bionic flexible pectoral fins in static water (as shown in Fig. 8) that the pectoral fins show large output propulsive force at all flapping frequencies when the flapping amplitude is 80°. However, there is no significant rise in the propulsive force with the increase in the flapping amplitude. Instead, the robot fish displays lower swimming stability due to the influence of the varying lift force.

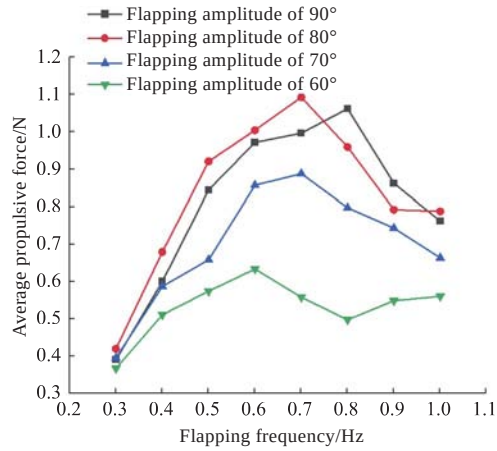

Fig. 8 Average propulsive force of the bionic pectoral fins under different drive parameters

In order to test the linear swimming speed of the prototype (XJRoman), this paper tests its average swimming speed at different drive frequencies of the pectoral fins with a flapping amplitude of 80°, and the results are presented in Fig. 9. The swimming speed measured in the test is expressed in a unit of body length per second (BL/s).

It is indicated from Fig. 9 that the flapping fre-

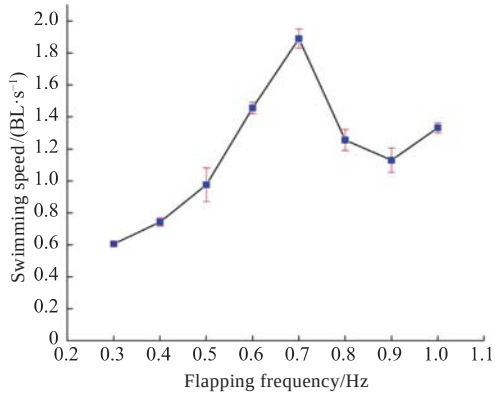

Fig. 9 Average swimming speed of the prototype at different flapping frequencies

quency has a significant influence on the swimming speed of the prototype. When the flapping frequency of the pectoral fins of the robot fish is lower than 0.7 Hz, the swimming speed of the prototype increases substantially with the rise in the flapping frequency of the pectoral fins and reaches the maximum value at 0.7 Hz, which is about 1.9 times the body length per second. When the flapping frequency of the pectoral fins exceeds 0.7 Hz, the average swimming speed of the prototype decreases as the flapping frequency of the pectoral fins increases. At a flapping amplitude of 80°, the changing trend of the linear swimming speed of the robot fish with the drive frequency is generally consistent with that of the average propulsive force of the bionic pectoral fins measured in the static water, and the maximum value occurs at a flapping frequency of 0.7 Hz.

2.3 Maneuverability tests

Fig. 10 (a) shows the motion image sequence of the myliobatid-inspired robot fish when it performs a side V-shaped maneuver. During swimming, the pectoral fins show the maximum flapping amplitude stable at 80° and a flapping frequency of 0.7 Hz and 0.5 Hz for the left and right pectoral fins, respectively, and the flapping frequency of the right pectoral fin is slightly smaller than that of the left one. By controlling the differential speed between the left and right pectoral fins of the robot fish, we increase the lift and propulsive forces generated by the pectoral fin on one side and thus provide rolling and yaw moments for the robot fish. Besides, we adjust the lift and drop amplitudes of the stern rudder to provide the robot fish with a pitch moment. The V-shaped maneuver successfully simulates the motion state of a real eagle ray when it is capturing its prey, and it can be applied to detect environments and collect samples in specific target waters.

Fig. 10 (b) shows the motion image sequence of the robot fish when it completes the rolling and hovering maneuvers. The whole process can be divided into three stages: accelerated climbing, rolling, and hovering. First, the robot fish reaches a certain depth at a growing speed by synchronously flapping the pectoral fins on both sides, and then it accelerates the flapping speed of the left pectoral fin to make its body heel to the right chord and finally coordinates the pectoral fins on both sides to make them synchronously but slowly flap, so as to perform stable hovering movement. In this test, the robot fish shows a hovering radius of about 0.5 m in the water and displays flexible maneuverability. The rolling and hovering maneuvers simulate the motion state of a real eagle ray when it is searching for its prey, and it can be applied to the reconnaissance and tracking of specific targets.

Fig. 10 (c) shows the motion sequence of the myliobatid-inspired robot fish when it dives and tumbles, and it can be observed that the robot fish tumbles and dives counterclockwise under the joint action of the propulsive force and the pitch moment provided by the stern rudder. The test results show that the robot fish can tumble at a large angle in the water under the coordinated efforts of the stern rudder and the pectoral fins, which thus show excellent vertical maneuverability.

(a) Side V-shaped maneuver

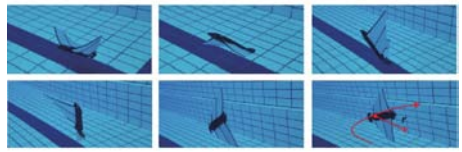

(b) Rolling and hovering maneuvers

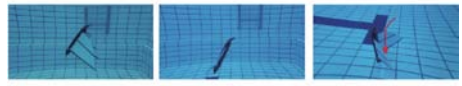

(c) Tumbling maneuver

Fig. 10 Sequence diagram of maneuverability tests on the myliobatid-inspired robot fish

3 Conclusions

Based on the anatomical characteristics of an eagle ray, this paper proposes an overall design of the prototype of a flap-driven myliobatid-inspired robot fish and produces the first-generation prototype. The prototype is driven by the fully flexible bionic pectoral fins and can control the pitch degree of freedom via the stern rudder. The low-density and high-toughness nylon (PA12) material is used to replace traditional metal materials to make the shell, which reduces the overall mass and ensures the underwater maneuverability of the prototype. The proposed CPG underlying drive method can well coordinate the periodic swing of the left and right pectoral fins and the stern rudder and enhance the stability of the prototype of the robot fish during swimming. Through the swimming performance test on the prototype of the bionic robot fish, it can be seen

that the change in the flapping frequency of the flexible pectoral fins on both sides has a significant influence on the swimming speed of the prototype when the flapping amplitude of the flexible pectoral fins is kept at 80°. Within a certain frequency range, an increase in the flapping frequency of the pectoral fins can enhance the average propulsive force output by the flexible bionic pectoral fins and thus improve the swimming speed of the prototype, with a maximum swimming speed of up to 1.9 times the body length per second. However, when the flapping frequency exceeds 0.7 Hz, an increase in the flapping frequency of the pectoral fins fails to effectively improve the swimming speed of the robot fish. Therefore, in the follow-up research, it is important to achieve the online monitoring and control of the flapping frequency of the flexible pectoral fins, so as to keep the prototype within an efficient range.

Besides, in the maneuverability tests, the flap-driven myliobatid-inspired robot fish designed in this paper can perform various agile underwater movements such as side V-shaped maneuver, rolling and hovering maneuvers, and tumbling maneuver, which displays excellent maneuverability. Therefore, the prototype can be widely applied in tasks such as underwater search and rescue, detection, and tactical strike.

References

[1] ZHANG Y H. Theoretic and experimental research on propulsion flexible biomimetic undulatory robotic fin [D]. Hefei: University of Science and Technology of China, 2008. (in Chinese)

[2] BANDYOPADHYAY P R. Trends in biorobotic autonomous undersea vehicles [J]. IEEE Journal of Oceanic Engineering, 2005, 30(1): 109−139.

[3] XU Y C, ZONG G H, BI S S, et al. Initial development of a flapping propelled unmanned underwater vehicle (UUV) [C]//2007 International Conference on Robotics and Biomimetics. Sanya: IEEE, 2008.

[4] GAO J, BI S S, XU Y C, et al. Development and design of a robotic manta ray featuring flexible pectoral fins [C]//2007 IEEE International Conference on Robotics and Biomimetics. Sanya: IEEE, 2008.

[5] ARASTEHFAR S, GUNAWAN G, YEO K S, et al. Effects of pectoral fins' spanwise flexibility on forward thrust generation [C]//2017 IEEE International Conference on Robotics and Biomimetics (ROBIO). Macau, Macao: IEEE, 2017.

[6] CHEW C M, LIM Q Y, YEO K S. Development of propulsion mechanism for Robot Manta Ray [C]//2015 IEEE International Conference on Robotics and Biomimetics. Zhuhai: IEEE, 2016.

[7] KIM H S, LEE J Y, CHU W S, et al. Design and fabrication of soft morphing ray propulsor: undulator and oscillator [J]. Soft Robotics, 2017, 4(1): 49−60.

[8] MOORED K W, FISH F E, KEMP T H, et al. Batoid fishes: inspiration for the next generation of underwater robots [J]. Marine Technology Society Journal, 2011, 45(4): 99−109.

[9] LAUDER G V, DRUCKER E G. Morphology and experimental hydrodynamics of fish fin control surfaces [J]. IEEE Journal of Oceanic Engineering, 2004, 29(3): 556−571.

拍动式仿鹞鳐水下机器人设计及其游动性能试验

郭松子*[1], 马俊[2], 李志印[1], 张进华[3]

1 中国舰船研究设计中心,湖北 武汉 430064

2 海军装备部 项目管理中心,北京 100071

3 西安交通大学 机械工程学院,陕西 西安 710049

摘　要:[**目的**]自然界中的鱼类经过长期的自然选择过程,进化出了各具特色的水中推进模式,具有推进效率高、机动性强与噪音低等优点,是水下航行器的理想仿生对象。为研制新一代低噪声、高机动性的自主水下航行器(AUV),以拍动推进的鹞鳐为仿生对象。[**方法**]通过分析其胸鳍内在的解剖结构,提出了一种采用对侧柔性胸鳍拍动推进的仿生机器人设计方案,并详述了实验样机本体的制作过程及其底层驱动控制方法。为测试机器鱼样机的游动性能,在实验水域中对所设计的原型样机展开了一系列游动性能测试。实验中测试了机器鱼样机在不同拍动频率下的游动速度,并在确定最大游动速度后,对其进行了机动性能测试。[**结果**]结果表明,所设计的实验样机能在水中完成包括翻滚、小半径转向与横滚盘旋在内的多种机动动作,其最大游动速度可达1.9倍体长每秒(约为0.73 m/s)。[**结论**]研究初步完成了拍动式仿鹞鳐水下机器人的设计与测试工作,为新一代高性能水下推进器的设计提供了一定的参考价值。

关键词:自主水下航行器;仿生机器人;游动性能试验